Spatially-resolved spectroscopic diagnosing of aluminum wire array Z-pinch plasmas on QiangGuang-I facility*

Ye Fan(叶 凡)[a)b)c)†], Li Zheng-Hong(李正宏)[a)], Qin Yi(秦 义)[a)], Jiang Shu-Qing(蒋树庆)[a)], Xue Fei-Biao(薛飞彪)[a)], Yang Jian-Lun(杨建伦)[a)], Xu Rong-Kun(徐荣昆)[a)], and Jin Yong-Jie(金永杰)[b)c)]

[a)] *Institute of Nuclear Physics and Chemistry, China Academy of Engineering Physics, Mianyang* 621900, *China*
[b)] *Key Laboratory of Particle and Radiation Imaging, Tsinghua University, Beijing* 100084, *China*
[c)] *Department of Engineering Physics, Tsinghua University, Beijing* 100084, *China*

(Received 26 May 2009; revised manuscript received 8 January 2010)

Spatially-resolved crystal spectrometers with a high spectral resolution are developed to diagnose K-shell x-ray radiation from Z-pinch plasmas. These diagnostic apparatuses are successfully applied to aluminum wire array Z-pinch experiments on QiangGuang-I facility, a driver with a pulsed current up to about 1.5 MA in 80 ns. Time-integrated experimental results show that the K-shell x-ray emission lines of aluminum Z-pinch plasmas are dominated by line emissions from helium-like ionisation state. Bright spots that might have higher electron temperature or density are produced randomly in location and size along the z-axis during implosions. According to the experimental data, the electron temperature and the ion density are estimated to be between 250 eV and 310 eV, and between 7.0×10^{19} cm^{-3} and 4.0×10^{19} cm^{-3} respectively, while the ion temperature is inferred to be about 10.2 keV, which is much higher than the electron temperature.

Keywords: Z-pinch, wire array, x-ray spectroscopy, spatially-resolved crystal spectrometer
PACC: 5255E, 5270L, 3220R

1. Introduction

The high temperature and high density plasmas produced by fast Z-pinch driven by pulsed-power facility are intense and efficient x-ray sources. By imploding a nested-wire array of several hundred fine tungsten wires with a current of 20 MA in 100 ns, Z accelerator[1] at Sandia National Laboratory has produced an x-ray power up to (280 ± 40) TW, with ∼15% conversion efficiency of input electrical energy into x-ray radiation.[2] Z-pinch of tungsten wire arrays,[3] which emits blackbody-like radiation, was recently applied to the research on inertial confinement fusion,[4,5] while Z-pinches of wire arrays made of low- to moderate-atomic number elements such as aluminum and titanium, which produce K-shell x-ray emissions, provide the opportunity for investigating x-ray spectrum, radiation transport and atomic physics analysis.[6−9]

In the study of Z-pinch plasma, x-ray spectroscopic diagnostics is widely used for the determination of plasma density and plasma temperature, which are of significance for radiation magnetohydrodynamic[10] and energy conversion mechanism analysis.[11] The electron density could be inferred from K-shell x-ray emission power[12] or from Stark broadening of line emission of Rydberg series.[13] The electron temperature could be determined by the ratio of K-shell line intensities or by the slope of x-ray continuum.[12,14] The ion temperature was mainly determined by Doppler broadening of line emissions.[13,15] It is noticeable that the broadening caused by other factors such as source size, opacity effect and Stark broadening should be carefully extracted, or one may choose a specific line, of which the width is dominated by Doppler broadening.[15] Ideally, these would be done with spatial and temporal resolutions simultaneously, but it is difficult to realise in practice. We develop two spatially-resolved crystal spectrometers and apply them to Z-pinch experiments. The spatially-resolved experimental data, even though not temporally-resolved, will give essential images of K-shell x-ray emissions from aluminum wire array Z-pinch plasmas.

2. Instrumentations

Two x-ray crystal spectrometers are designed and built to obtain highly spectrally-resolved x-ray im-

*Project supported by the National Natural Science Foundation of China (Grant No. 10635050).
†Corresponding author. E-mail: yefan1931@126.com
© 2010 Chinese Physical Society and IOP Publishing Ltd

ages of aluminum wire array implosions. One is a convex curved crystal spectrometer; the other is a spherically bent crystal spectrometer. Ray-tracing programs and computer-assisted drawings (CADs) are used for analysing the performances of the spectrometers and giving proper structures and layout on the QiangGuang-I facility.

In the convex curved crystal spectrometer, the dispersion unit is a cylindrically bent mica crystal, with the crystal lattice spacing $2d = 19.84$ Å (1 Å = 0.1 nm) and the curvature radius 60 mm. X-rays from the source are dispersed from the crystal according to the Bragg equation $2d \sin\theta = n\lambda$, where n is the reflection order. In experiments, its dispersion plane is set to be perpendicular to the z-axis. Between the x-ray source and the crystal, a 100-μm-wide slit is located in the direction perpendicular to the z-axis to give a spatial resolution along the z-axis. An x-ray film, which records spectra reflected by crystal, is curved with a radius of 120 mm and its centre is placed at a position(0 mm, 50 mm). The x-ray source is located at a position (–500 mm, 0 mm). A beryllium foil with a thickness of 15 μm is used as a filter to shield the visible light and plasma debris. Here, the curvature centre of the cylindrically bent crystal is assumed to be at a position (0 mm, 0 mm). Figure 1 shows the calculated spectral broadening caused by three different mechanisms. The instrumental broadening is determined by the rocking angle of the crystal. The line broadening is specified as $\Delta\lambda/\lambda = 1.05 \times 10^{-3}$, corresponding to a Doppler broadening at ion temperature $T_{\rm i} = 5$ keV. The source size broadening is obtained by assuming the source size to be 2.0 mm in diameter. It is shown that the spectral broadening is mainly caused by source size broadening in convex curved crystal spectrometer, which gives an opportunity to recover the source size by spectral width. These results lead to a spectral resolution ($\lambda/\Delta\lambda$) of 200 at a wavelength of 7.17 Å.

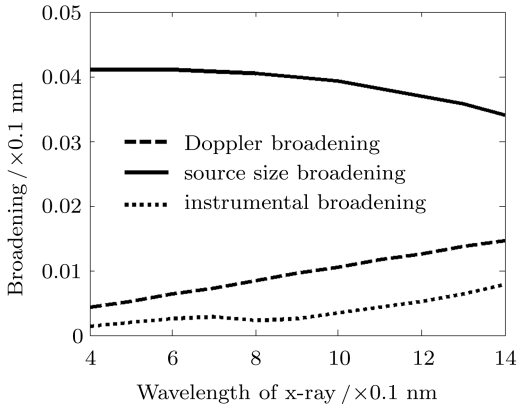


Fig. 1. Curves for line broadening, source size broadening and instrumental broadening versus wavelength of x-ray for the convex curved crystal spectrometer.

In the spherically bent crystal spectrometer, the detector is so arranged that this spectrometer can serve as a focusing spectrograph with a two-dimensional (2D) spatial resolution (see Fig. 2), which is usually referred as focusing specrograph with 2D spacial resolution (FSSR-2D).[16] The x-ray source is placed at a distance of 1300 mm from the centre of crystal (point C in Fig. 2) and the grazing angle of x-rays incident at the centre of crystal was 49°. The broadening effects for this spectrometer are displayed in Fig. 3, showing that line broadening is a main factor causing spectral broadening when the spectrum on the detector is located not very far from the Rowland circle. The calculated spectral resolution($\lambda/\Delta\lambda$) at a wavelength of 7.17 Å is about 890. The filter is composed of a 20-μm-thick polystyrene and 4-μm-thick titanium.

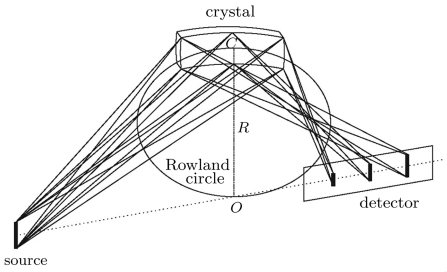


Fig. 2. Diagram of the focusing spectrograph with a 2D-spatial resolution with using a spherically bent crystal.

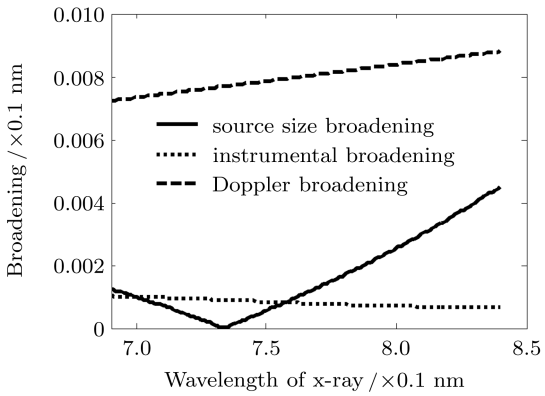


Fig. 3. Curves for line broadening, source size broadening and instrumental broadening versus wavelength of x-ray in FSSR-2D. The minimum of source size broadening (solid line) corresponds to the case where the spectrum is at the cross point of the detector and the Rowland circle.

3. Experimental results

Experiments were carried out on a QiangGuang-I pulse power generator, a ∼1.5 MA Z-pinch driver with a rise time of about 80 ns. The load, composed of an annular array of 32 15-μm-diameter aluminum wires, had a radius of 4 mm, a length of 20 mm and a total mass of 309 μg.

Several typical time-integrated x-ray spectra of aluminum Z-pinch plasmas on QiangGuang-I facility are shown in Figs. 4 and 5. In these figures, the horizontal direction is the dispersion direction, while the

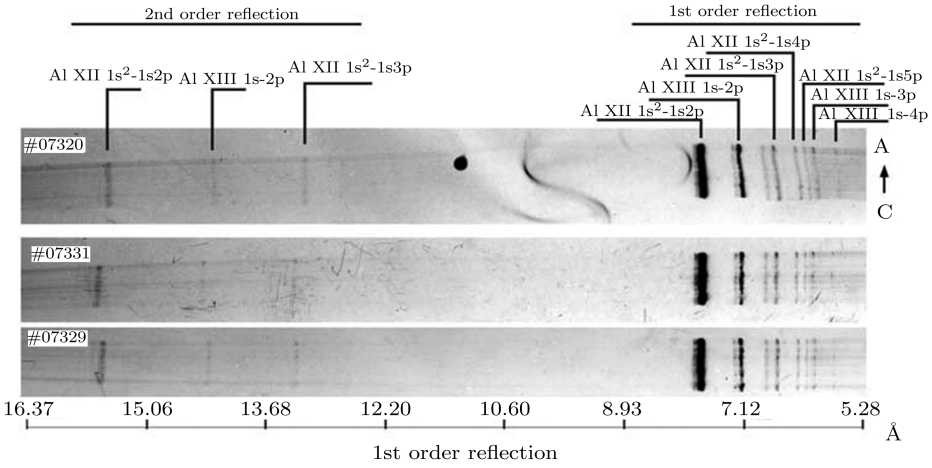


Fig. 4. Spectra recorded by the convex curved crystal spectrometer.

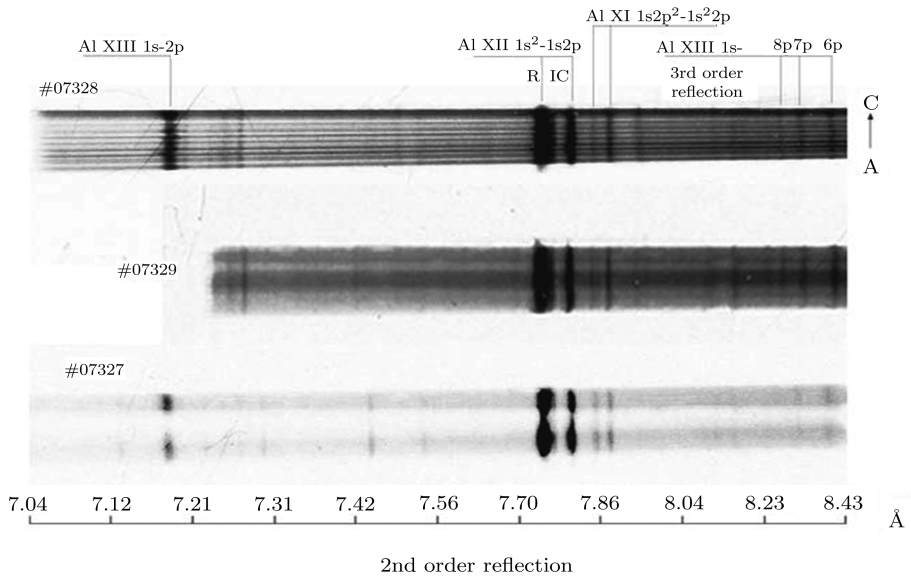


Fig. 5. Spectra recorded by the spherically bent crystal spectrometer.

vertical direction is parallel to the pinch axis and is spatially resolved. Ion levels involved in the transitions giving rise to the line are labeled above the spectra, and the anode and cathode are denoted as A and C in the figures respectively. It is clearly seen that lines from the He-like ionisation state (Al XII) are the most intense. Lines from H-like ions (Al XIII) are also visible. Another feature of the spectra is the presence of x-ray continuum emitted from some local area (called 'bright spots') along the z-axis. These bright spots are varied in size and location along the z direction from shot to shot, and also nonuniformly distributed in a single shot. In Fig. 5, spectra of shot No. 07328 show that the bright spots are almost uniformly distributed along the z direction with size $\delta z \approx$ 1 mm except that located at the cathode, while bright

spots in shot No. 07327 are mainly located at the cathode and the anode with size $\delta z \approx 4$ mm. The slope of the x-ray continuum could be used for inferring the electron temperature. However, it is difficult to characterise the intensity versus wavelength profile because any point on the continuum may result from many different order Bragg reflections due to the higher order (from 2nd order to 13th order) reflections of mica crystal. Spectra of shot No. 07327 in Fig. 5 show that Al XII $1s^2$-1s2p is emitted from the entire length of the pinch, including at axial positions where there was no continuum. However, some lines, such as Al XIII 1s-2p and 1s-6p appear only at axial positions where there was intense continuum. This may be a result of either higher electron temperature or higher density in the bright spots than elsewhere.

The values of practical spectral resolution ($\lambda/\Delta\lambda$) of the convex crystal spectrometer and the spherically bent crystal spectrometer can be estimated by spectral broadening: for wavelength at 7.17 Å (Al XIII 1s-2p), they are $7.17/0.04 \approx 179$ and $7.17/0.012 \approx 598$ respectively.

In order to estimate the electron temperature and the electron density, a set of data, including the plasma size given by a pinhole camera filtered by 4-μm-thick titanium foil, the K-shell x-ray power given by the filtered x-ray power meter and the line intensity ratio from the spectra, are analysed. Taking into consideration the responses of the x-ray film and filters, we obtain from shot No. 07329 in Fig. 4 that Lyβ/Heβ = 0.13. The plasma size is obtained to be about 2.0 mm from the filtered x-ray pinhole image. Meanwhile the keV x-ray power is measured to be about 0.1 TW/cm at the stagnation. The electron temperature and the ion density are estimated based on detailed collisional radiative equilibrium calculations[6] to be between 250 eV and 310 eV, and between 7.0×10^{19} cm^{-3} and 4.0×10^{19} cm^{-3}, respectively. The ion temperature is inferred by the Doppler width of helium-like intercombination line (denoted as IC in Fig. 5) that is free of opacity broadening and Stark broadening.[15] Figure 6 shows its line shape of shot No. 07329. The ion temperature is inferred to be about 10.2 keV from the line width, with the source size broadening extracted. Time-integrated results show that the ion temperature is much higher than the electron temperature. Till now, we are still not very clear about the mechanisms that lead to this result.

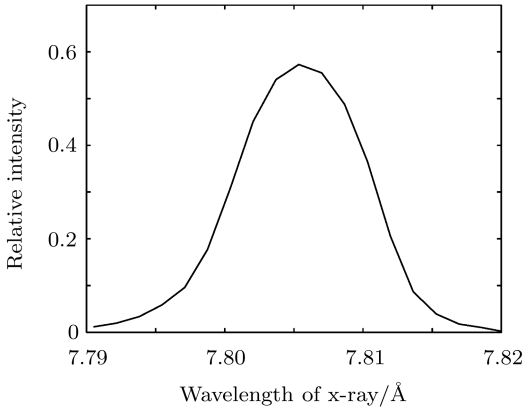


Fig. 6. Line shape of helium-like intercombination line(Al XII 1s2p ^{3}P→1s^2 ^{1}S).

4. Conclusions

The highly resolved spectroscopic diagnostic systems are developed and applied to Z-pinch experiments on QiangGuang-I facility successfully. The time-integrated results show their appropriateness and capability in exploring the plasma parameters. We pay much attention to its spatial resolution because of the nonuniformity of Z-pinch plasmas, caused by the magnetohydrodynamic instabilities. Temporally-resolved results obtained with the updated diagnostics can present more information about the implosion dynamics and the ionisation dynamics in the future.

References

[1] Spielman R B, Deeney C, Chandler G A, Douglas M R, Fehl D L, Matzen M K, McDaniel D H, Nash T J, Porter J L, Sanford T W L, Seamen J F, Stygar W A, Struve K W, Breeze S P, McGurn J S, Torres J A, Zagar D M, Gilliland T L, Jobe D O, McKenney J L, Mock R C, Vargas M, Wagoner T and Peterson D L 1998 *Phys. Plasmas* **5** 2105

[2] Deeney C, Douglas M R, Spielman R B, Nash T J, Peterson D L, L'Eplattenier P, Chandler G A, Seamen J F and Struve K W 1998 *Phys. Rev. Lett.* **81** 4883

[3] Xu R K, Li Z H, Yang J L, Xu Z P, Ding N, Guo C, Jiang S L, Ning J M, Xia G X, Li L B, Song F J and Chen J C 2005 *Chin. Phys.* **14** 1613

[4] Vesey R A, Herrmann M C, Lemke R W, Desjarlais M P, Cuneo M E, Stygar W A, Bennett G R, Campbell R B, Christenson P J, Mehlhorn T A, Porter J L and Slutz S A 2007 *Phys. Plasmas* **14** 056302

[5] Bailey J E, Chandler G A, Slutz S A, Golovkin I, Lake P W, MacFarlane J J, Mancini R C, Burris-Mog T J, Cooper G, Leeper R J, Mehlhorn T A, Moore T C, Nash T J, Nielsen D S, Ruiz C L, Schroen D G and Varnum W A 2004 *Phys. Rev. Lett.* **92** 085002

[6] Apruzese J P, Whitney K G, Davis J and Kepple P C 1997 *J. Quant. Spectrosc. Radiat. Transfer* **57** 41

[7] Jones B, Deeney C, Coverdale C A, LePell P D, Mckenney J L, Apruzese J P, Thornhill J W, Whitney K G, Clark R W, Velikovich A L, Davis J, Maron Y, Kantsyrev V, Safronova A and Oreshkin V I 2006 *J. Quant. Spectrosc. Radiat. Transfer* **99** 341

[8] Apruzese J P, Davis J, Whitney K G, Thornhill J W, Kepple P C, Clark R W, Deeney C, Coverdale C A and Sanford T W L 2002 *Phys.Plasmas* **9** 2411

[9] Bailey J E, Chandler G A, Cohen D, Cuneo M E, Foord M E, Heeter R F, Jobe D, Lake P W, MacFarlane J J, Nash T J, Nielson D S, Smelser R and Torres J 2002 *Phys. Plasmas* **9** 2186

[10] Sanford T W L, Nash T J, Mock R C, Spielman R B, Struve K W, Hammer J H, De Groot J S, Whitney K G and Apruzese J P 1997 *Phys. Plasmas* **4** 2188

[11] Kroupp E, Osin D, Starobinets A, Fisher V, Bernshtam V, Maron Y, Uschmann I, Forster E and Deeney C 2007 *Phys. Rev. Lett.* **98** 115001

[12] Whitney K G, Thornhill J W, Pulsifer P E, Apruzese J P, Sanford T W L, Nash T J, Mock R C and Spielman R B 1997 *Phys. Rev.* E **56** 3540

[13] Wong K L, Springer P T, Hammer J H, Iglesias C A, Osterheld A L, Foord M E, Bruns H C, Emig J A and Deeney C 1998 *Phys. Rev. Lett.* **80** 2334

[14] Sanford T W L, Nash T J, Mock R C, Spielman R B, Seamen J F, McGurn J S, Jobe D, Gilliland T L, Vargas M, Whitney K G, Thornhill J W, Pulsifer P E and Apruzese J P 1997 *Rev. Sci. Instrum.* **68** 852

[15] Yadlowsky E J, Barakat F, Carlson E P, Hazelton R C, Keitz M, Klepper C C, Failor B H, Levine J S, Song Y, Whitten B L, Coverdale C R, Deeney C and Spielman R B 2002 *J. Appl. Phys.* **92** 3458

[16] Pikuz T A, Faenov A Y, Pikuz S A, Romanova V M and Shelkovenko T A 1995 *J. X-ray Sci. Tech.* **5** 323